Received: April 27, 2022. Revised: June 23, 2022.

INASS

International Journal of
Intelligent Engineering & Systems

http://www.inass.org/

Premature Ventricular Contraction Classification Based on Spiral Search - Manta Ray Foraging and Bi-LSTM

Sharada Suresh Dambal[1]* Mahesh Kumar Doddananjedevaru[2]
Sudarshan Budnur Gopalakrishna[1]

[1]RV College of Engineering, Bengaluru 560059, India
[2]JSSATE, Bengaluru 560060, India
* Corresponding author's Email: sharu041@gmail.com

Abstract: Cardiovascular Diseases (CVDs) have become a burden to the healthcare system due to the increase in the number of patients and the ratio of mortality. Various techniques are applied for the classification of Premature Ventricular Contraction (PVC) and existing methods have lower sensitivity due to more similarity of features between classes. This research proposes the Spiral Search - Manta Ray Foraging (SP-MRF) algorithm to select the unique features that help to increase the sensitivity of the model. The Convolutional Neural Network (CNN) based model is used for the feature extraction from the input signals and the SP-MRF method selects features from extracted features. The Spiral Search technique increases the exploitation of the search method that helps to distinguish between more similar features and select unique features for classes. The selection of unique features helps to increase the sensitivity and efficiency of the model in PVC classification. The selected features were applied for the Bi-directional Long Short Term Memory (BiLSTM) for PVC classification and evaluated the performance. The efficiency of the SP-MRF-BiLSTM model is evaluated on the MIT-BIH dataset for PVC classification. The SP-MFR-BiLSTM model has 99.97 % accuracy, and 99.52 % sensitivity and the KNN-deep metric has 99.59 % accuracy and 96.7 % sensitivity in the model.

Keywords: Bi-directional long short term memory, Cardiovascular diseases, Convolutional neural network, Premature ventricular contraction, Spiral search - manta ray foraging.

1. Introduction

Recently, Cardiovascular Diseases (CVDs) have greatly increased worldwide and CVDs is considered one of the leading cause of death in many countries. Electrocardiograms (ECG) provide a measure of non-invasive heart electrical activity and are commonly used to monitor and assess the cardiac status of a patient [1]. Rheumatic heart disease, cerebrovascular illness, coronary heart disease, blood vessel disorders and other disease-related to the heart are known as CVDs. Strokes and Heart attacks are responsible for more than four out of every five CVD fatalities, with one-third of these deaths occurring before 70 [2]. Arrhythmia is a heart condition that characterizes based on heartbeat rhythm or rate and the heartbeat is faster than normal, has an irregular pattern, or is too slow. Commonly known cardiovascular diseases include arrhythmias types such as Premature Ventricular Contraction (PVC), Premature Atrial Contraction (PAC), Ventricular Fibrillation (VF), and Atrial Fibrillation (AF) [3]. Arrhythmia classification based on Electrocardiogram (ECG) is required for diagnosis and heart diseases prevention. In the bio-signal analysis field, ECG signals classification receives the most attention. Cardiologist faces the problem of accurate diagnosis of a large number of ECG signal due to the complexity of ECG records. Automatic classification of arrhythmia is an effective way to reduce the burden on cardiologists [4, 5].

Arrhythmia detection based on intelligent systems are applied to overcome such disadvantages that involve techniques such as machine learning,

statistical analysis, and biomedical signal processing. Statistical analysis and signal processing are widely applied to extract distinguishing features that better depict the ECG signal characteristics and ECG system reveals dynamics [6, 7]. Premature Ventricular Contractions (PVCs) are often based on Idiopathic ventricular arrhythmias. PVCs commonly occur without structural heart disease and present with a focal mechanism. The activation from PVC origin from such a setting propagate normally through the healthy myocardium and provides characteristic of ECG, which are specific to the PVC origin site [8, 9]. Monitoring through Holter for this purpose is often used and computational tools provide essential assistance to specialists. The existing methods were applied for PVC detection based on QRS complexes and feature selection methods [10]. The objectives and contribution of this research are discussed as follows:

The spiral search is proposed in the MRF method to improve the exploitation of the model and increases the efficiency of the PVC classification. The SP-MRF method selected features that are applied to the BiLSTM model for the classification of PVC.

The spiral search technique selects the unique features for the classification due to its ability to distinguish more similar features. This advantage helps to improve the sensitivity of the model in PVC classification.

The SP-MFR-BiLSTM model is compared with existing methods in PVC classification, individual feature selection and classification. The SP-MFR-BiLSTM model shows higher efficiency in PVC classification than existing models.

The paper is organized as follows: Literature reviews related to the existing research works are explained in Section 2 and the SP-MRF-BiLSTM model is illustrated in Section 3. The simulation setup is given in Section 4 and the results & discussion are illustrated in Section 5. The conclusion of this research work is given in Section 6.

2. Literature review

Cardiac arrhythmia is very complex to handle for the hospitals due to increases in number of patients and ratio of mortality. Some of the research involves in applying the machine learning based methods for Premature Ventricular Contraction was reviewed in this section.

Mastoi [11] applied derived variables from ECG signals such as verification of P-wave, QRS duration, R-R wave interval, and interval of previous R-R wave. Applied four classifiers such as Random Forest (RF), Naïve Bayes (NB), Support Vector Machine (SVM) and K-Nearest Neighbor (KNN). The notch filter is applied to the band rejection filter to eliminate power line interference and high frequency noise from a signal. The developed model was evaluated using MIT-BIH-AR dataset for the classification of signal. The windowing algorithm was applied to set window for intervals with zero value of particular interval. The KNN model is sensitive to outlier and SVM model has imbalance data problem.

Wang [12] applied Convolutional Neural Network (CNN) model to clinical ECG reports of scanned ECG images to segment and classify the heartbeats. The OTSU algorithm was applied with erosion and dilation. The CNN-based model was evaluated using Fujian Provincial Hospital data and the MIT-BIH dataset to test its efficiency. The OTSU algorithm and gamma transform were applied for automatic extraction of ECG signal and to differentiate the curve. The development of a classification model and automatic heartbeat segmentation for a normal heartbeat and Premature Ventricular Contraction (PVC) were carried out. The heartbeat was segmented and classified after the ECG curve extraction. CNN training requires large data and training the CNN model causes overfitting problems due to the generation of more features in network.

Sarshar [13] applied deep learning based PVC recognition model and evaluate the model using the MIT-BIH dataset. Three morphological features in statistical features such as QRS width, QR amplitude, RS amplitude, and 10 heartbeats. Each signal is computed with seven statistical features in the classification model. ECG data of 20 s was used to extract the features that create a feature vector. CNN model was applied with these features to classify and find unique patterns more effectively for the network. The pipeline model improves the efficiency of arrhythmia diagnosis and is evaluated using of MIT-BIH dataset. The CNN model generates more features in the network and is applied with extra features causing an overfitting problem.

Yu [14] applied a PVC detection model from long-term ECG signal and utilize deep metric learning to extract features with a separated inter-product difference and compact intra-product variance. Sample distance calculated using KNN classifier based on these features is used to detect PVC in the system. Supervised deep metric learning performs automatic feature extraction that avoids bias in the system. The KNN-based classifier was evaluated using the MIT-BIH dataset for the classification of PVC. The deep model features

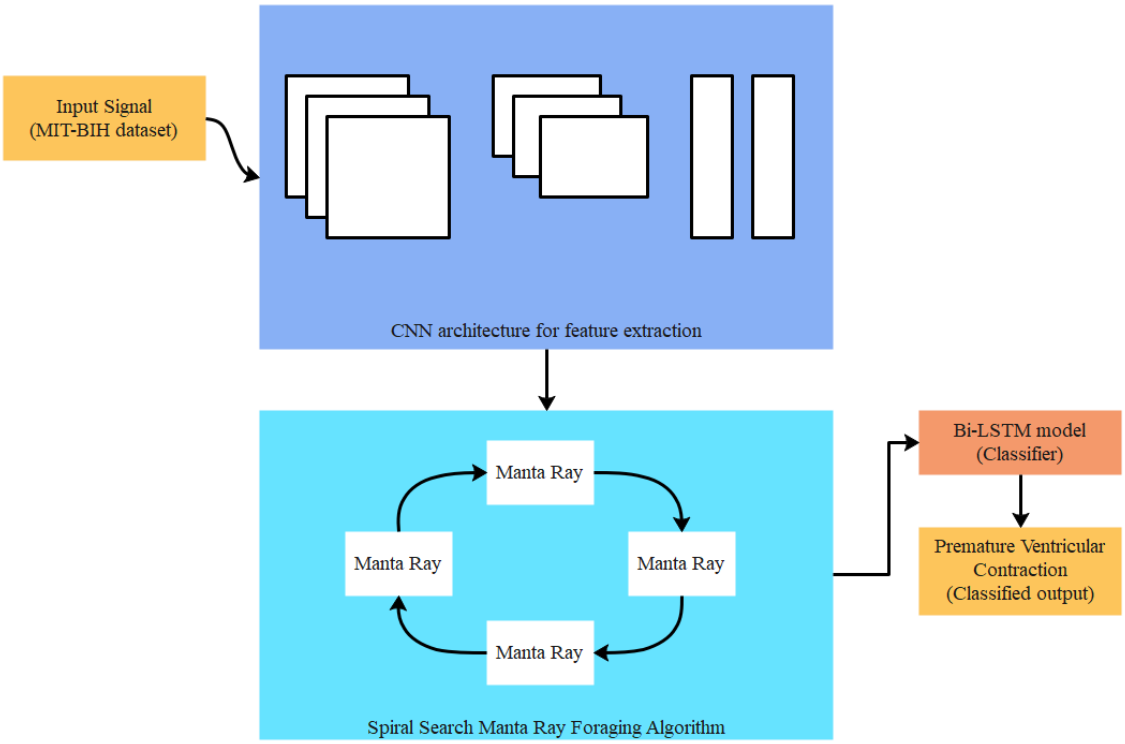

Figure. 1 The flow of the SP-MRF model in PVC classification

consist of outlier data and the KNN model is sensitive to outlier data that affects the efficiency of the model.

Yang [15] applied an ensemble classifier model for heart ventricular and atrial abnormalities detection in ECG signals based on morphological features. The ECG signal was pre-processed to detect the main character waves in the input signal. Selected ECG segments extraction and ECG morphological features combination were used for classification. The features such as wavelet decomposed ECG signal, principal components of the third and fourth level, QRS complex of morphological visual pattern, and morphological parameters were applied in the model. Several popular classification models knowledge is integrated for the ensemble classification method. The ensemble model is evaluated using AAMI standards and the MIT-BIH dataset. The ensemble model has a limitation of voting-based selection that affects the sensitivity of the model.

3. Proposed method

This research proposes the SP-MRF method for the feature selection process that improves the classification of PVC. The CNN model is applied for feature extraction and SP-MRF model selects features from CNN features. The selected features are applied to the Bi-LSTM model for the classification. The flow of SP-MRF model is shown in Fig. 1.

3.1 Convolutional neural network

The CNN model consists of Convolutional layer, pooling layer, and output layer for feature extraction from the signal.

3.2 Convolutional layer

The CNN model gained popularity in various domains due to its capacity to learn a representation of images [19, 20]. CNN model consists of convolutional layers that apply kernels convolution in input data to learn features from input data. The non-linear activation function is applied to perform a filter, as given in Eq. (1).

$$a_{i,j} = f\left(\sum_{m=1}^{M}\sum_{n=1}^{N} w_{m,n} \cdot x_{i+m,j+n} + b\right) \quad (1)$$

Where bias value is denoted as b, a non-linear function is denoted as f, convolution weight matrix is denoted as $w_{m,n}$, the corresponding activation is denoted as $a_{i,j}$, neuron (i,j) connected to upper neurons denoted as $x_{i+m,j+n}$.

Rectified Linear Unit (ReLU) of convolution layers are applied to measure feature maps and non-linear functions, as given in Eq. (2).

$$\sigma(x) = max\ (0, x) \quad (2)$$

CNN model consists of more convolution kernels and input samples are used to mine more hidden features. CNN model has been applied with two convolution layers. Feature extraction is carried out based on 64 convolutional kernels and the first convolutional layer is used for the 1 × 5 convolution kernel. The deeper feature extraction is carried out based on 128 convolution kernels and the convolution window is carried out based on 2 sliding steps. The 1 × 3 sizes of each convolution kernel were applied and layer is applied with convolution window of 1 step size. Two convolutional layers are applied with a Max-pooling layer to perform down-sampling. The filter noise interference is applied with two processes and the dominant feature is applied to reduce features.

3.2.1. Pooling layer

The computational burden and overfitting problems are provided by an activation map of many features in the system. Non-linear sub-sampling in the pooling layer is performed to minimize the features in the system. Translation invariance is carried out by pooling and two pooling methods are commonly used such as max-pooling and average pooling. In each pooling region, max pooling is used with max value and average pooling is used with the average value.

3.2.2. Output layer

The output layer is applied with a softmax classifier and a fully connected layer in the system. A fully connected layer is used as the last layer that is used to extract features from the network. A fully connected layer of each node is connected with upper layer nodes to merge extracted features.

3.3 Manta ray foraging optimization

Manta Ray Foraging optimization mimics the Manta Ray Behaviour [16-18]. Main foraging strategies such as somersault, cyclone, and chaining are formulated in the MRFO method. MRFO method is similar to several metaheuristic algorithms and randomly defined initialization is given in Eq. (3).

$$X_{i,j}(t) = Lb_{i,j} + r(:).\left(Hb_{i,j} - Lb_{i,j}\right)$$

$$\forall i \in N_{pop}, j \in N_{var} \quad (3)$$

Chaining strategies of best foodstuffs are applied in Manta Ray behaviour to change the positions ($X_{i,j}$) [16].

$$\alpha = 2.r(:).\sqrt{\left|log\left(r(:)\right)\right|} \quad (4)$$

Spiral similar to swarm swimming to cyclones is carried out based on foodstuff noticing. In this operator, the Positions of the latest Manta Ray are adjusted around the best position, as in equation (5).

$$X_{i,j}(t+1) = X_{i,j}(t) + SF.\left(r_2 X_{best,j} - r_3 X_{i,j}(t)\right) \forall i \in N_{pop} \quad (5)$$

Where high food concentration of best location *j* is defined as X_{best} [16].

$$\beta = 2.exp\left(r_1.\frac{T_{max}-t+1}{T_{max}}\right).sin\,(2\pi r_1) \quad (6)$$

If verified the low concentration, the random position is set [16].

Two specific behaviors such as exploration and exploitation are set in the method. Specific operators are used to balance exploration and exploitation in metaheuristic algorithms. If t/T_{max} in MRFO is less than rand, then exploitation cycle is performed otherwise search space is performed. The MRFO control system performs SF, N_{pop},and T_{max} that is followed to ensure good performance.

3.3.1. Spiral search technique

The Manta Ray second state is randomly generated to a position in the space. The blind operation of this kind slows down algorithm convergence speed. The spiral search mechanism is introduced to solve this problem. The spiral search mechanism has more possibilities for Manta ray to make full use of location thus increasing global solution ability in the optimization process. The spiral structure trajectory was applied as a search space which is measured based on a calculation of the distance between Manta Ray best position and the previous position. The mathematical expression is given as follows in Eq. (7).

$$x^{t+1} = D.exp(b \times l).cos(2\pi l) + gbest \quad (7)$$

Where l denotes a random number in a range of [-1, 1], the logarithmic spiral shape is defined as a constant b, the distance from current best position from i^{th} position of Manta Ray is denoted as $D = |gbest - x_i^t|$.

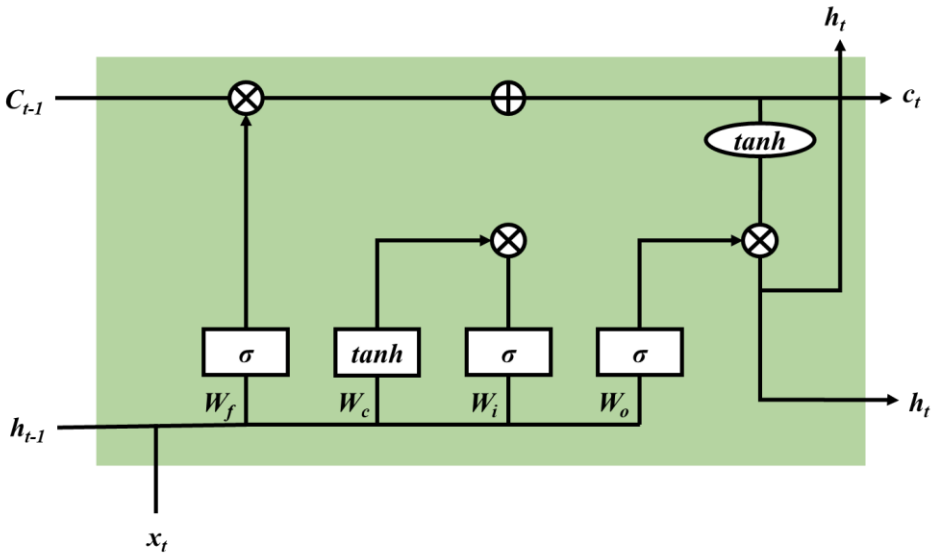

Figure. 2 The architecture of the long short term memory (LSTM) model

3.4 Bi-LSTM

The LSTM model decides the features be discarded or stored in long term. CVD classification requires historic data and recent data for effective classification. The self-feedback method is applied in LSTM model with a hidden layer to handle dependence problem in long-term [19, 20].

Memory cells and three gates are used to store features in LSTM model that handles long-term features problem. The architecture of LSTM unit is shown in Fig. 2.

The cell output is denoted as h_t, cell value memory is denoted as c_t, the previous step of cell output is denoted as h_{t-1} and input data at time t is denoted as x_t. The step by step process of LSTM unit is denoted as follows.

The LSTM unit output h_t is measured, as given in Eq. (8).

$$h_t = o_t \times tanh\,(c_t) \tag{8}$$

The weight matrix is denoted as W_0, the bias is denoted as b_0, the memory cell of control state value is o_t, and output gate o_t is given in Eq. (9).

$$o_t = \sigma(W_0.[h_{t-1}, x_t] + b_0) \tag{9}$$

The LSTM unit last state value is denoted as c_{t-1} in memory cell c_t of the current moment, as in Eq. (10).

$$c_t = f_t \times c_{t-1} + i_t \times \tilde{c_t} \tag{10}$$

Where dot product is denoted as "×". The last cell and candidate cell state values are used by the memory cell to control the input and output gate.

Forget gate controls historical data in memory cell state value, the forget gate is denoted as f_t, the bias is denoted as b_f, the weight matrix is denoted as W_f. The forget gate process is given in Eq. (11).

$$f_t = \sigma(W_i.[h_{t-1}, x_t] + b_f) \tag{11}$$

Memory cell state value of current input data update input gate, the input gate is denoted as i_t, the weight matrix is denoted as W_i, sigmoid function is denoted as σ, and the bias is denoted as b_i. The input gate process is given in Eq. (12).

$$i_t = \sigma(W_i.[h_{t-1}, x_t] + b_i) \tag{12}$$

Eq. (13) denotes candidate memory cell $\tilde{c_t}$, bias is denoted as b_c and weight matrix is denoted as W_c.

$$\tilde{c_t} = tanh\,(W_c.[h_{t-1}, x_t] + b_c) \tag{13}$$

LSTM model memory cell and control gates in model perform long term information store and update. LSTM model control output dimension that uses weight matrix adjust based on internal parameters.

The Bi-LSTM model consists of two LSTMs with each token of sequence learning applied for tokens based on past and future content. The Bi-LSTM model processes data in two manners: left to right and right to left. Hidden unit function $\vec{h}$ at a hidden forward layer is used for the forwarding process and at each time step t of the previous hidden state h_{t-1}

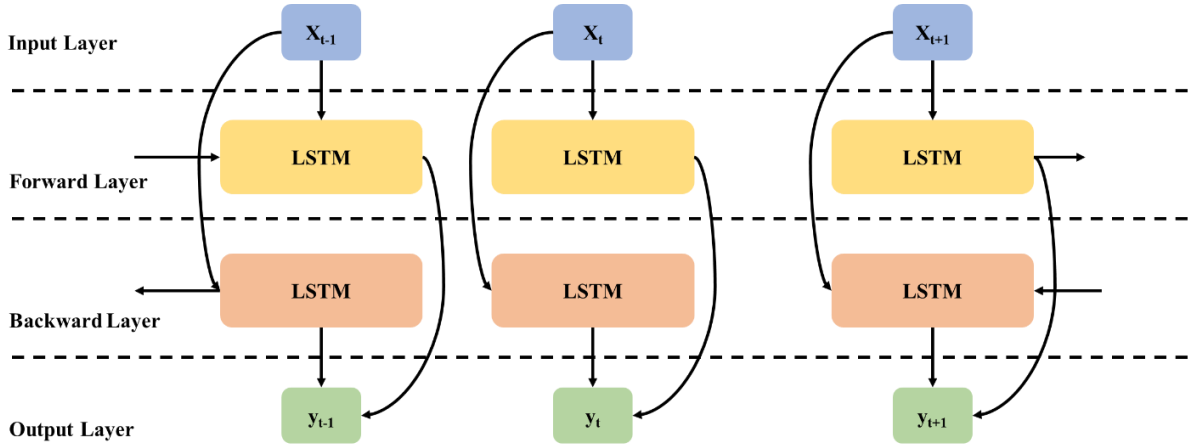

Figure. 3 The overview of BiLSTM model

is used for the reverse process. Hidden backward layers are used by a hidden unit function $\overleftarrow{h}$ and future hidden state $\overleftarrow{h}_{t+1}$. The concatenate $\overleftarrow{h}_t$ and $\vec{h}_t$ to create a long vector to represent forward and backward process of content representation. Combined output classification is used for target class. The Bi-LSTM model overview is shown in Fig. 3.

4. Simulation setup

Dataset: The public benchmark MIT-BIH arrhythmia dataset [21] is used to evaluate the model performance in arrhythmia classification. The dataset consists of 48 two-lead recordings and each consists of 30 minutes duration.

Parameter settings: In the Bi-LSTM model, the number of epochs is set as 8, the number of the hidden layer is set as 150, dropout is set as 0.2 and adam optimizer is used as the network optimizer. In SP-MRF, the number of iterations is set as 50 and the number of population is set as 50.

System Configuration: The SP-MRF model for PVC detection is carried out in a system of 16 GB RAM, 6 GB graphics card and Intel i7 processor.

Metrics: The accuracy, precision and recall formula is given in Eqs. (14) to (16).

$$Accuracy = \frac{TP+TN}{TP+TN+FP+FN} \times 100 \quad (14)$$

$$Precision = \frac{TP}{TP+FP} \times 100 \quad (15)$$

$$Recall = \frac{TP}{TP+FN} \times 100 \quad (16)$$

5. Results

The SP-MRF-BiLSTM model is applied for the classification of PVC and evaluated in MIT-BIH dataset. The performance metrics and error values are calculated in the model and discussed in this section.

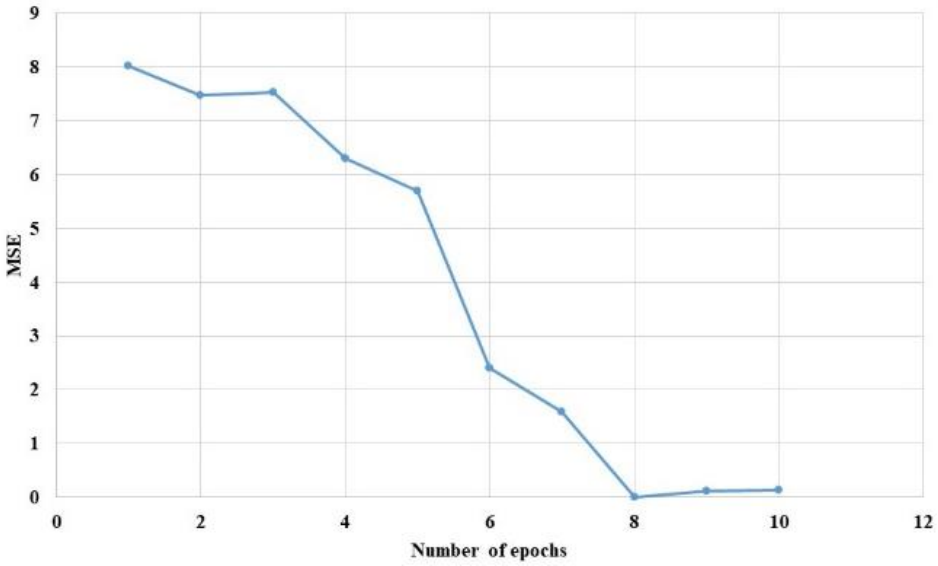

Figure. 4 The error value measures vs number of epochs

Table 1. Feature selection methods in PVC detection

Methods	Accuracy (%)	Sensitivity (%)	Specificity (%)
WOA	89.4	88.3	87.6
GO	92.3	90.3	91.1
MRF	95.3	91.2	92.1
SP-MRF-BiLSTM	99.97	99.52	99.4

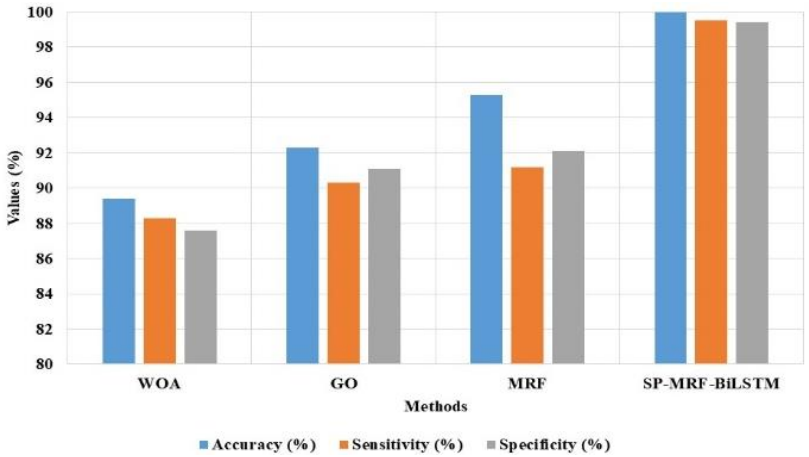

Figure. 5 Feature selection analysis on MIT-BIH dataset

Table 2. Classifier analysis in PVC classification

Methods	Accuracy (%)	Sensitivity (%)	Specificity (%)
KNN	84.1	83.6	84.5
SVM	89.4	84.2	83.8
RF	88.7	87.2	86.5
LSTM	98.7	97.3	98.2
SP-MRF-BiLSTM	99.97	99.52	99.4

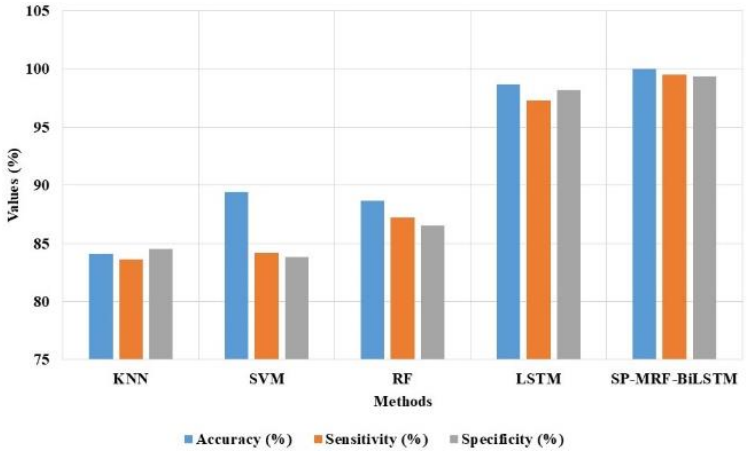

Figure. 6 Classifier analysis on PVC classification

Table 3. Comparative analysis in PVC classification

Methods	Accuracy (%)	Sensitivity (%)	Specificity (%)
Hybrid feature extraction [11]	99.96	98.9	99.2
OTSU - Gamma [12]	98.25	95.47	97.72
Deep learning based PVC [13]	N/A	99.2	N/A
KNN-deep metric [14]	99.59	96.7	96.7
Ensemble classifier [15]	98.68	N/A	N/A
SP-MRF-BiLSTM	99.97	99.52	99.4

Error value is calculated for various numbers of epochs in the SP-MRF-BiLSTM for classification of PVC, as shown in Fig. 4. The MSE value is reduced for 8 epochs due to increases of learning in the network. In 9th and 10th epochs, error value increases due to an overfitting problem in the network.

The SP-MFR-BiLSTM model is evaluated on MIT-BIH dataset for feature selection and compared with existing feature selection methods, as given in Table 1 and Fig. 5. The SP-MRF-BiLSTM model provides higher efficiency in terms of accuracy, sensitivity and specificity due to the increase in exploitation of the SP-MRF-BiLSTM model. The SP-MRF-BiLSTM model balance the trade-off between exploration and exploitation in search which helps to increase efficiency. The spiral search helps to find the unique features and increases the sensitivity of the model. The WOA and GO model has giving priority to local features that involve in local optima trap. The SP-MRF-BiLSTM model has 99.97 % accuracy, and 99.52 % sensitivity and MRF method has 95.3 % accuracy and 91.2 % sensitivity.

The SP-MFR-BiLSTM model is compared with the existing classifier in PVC classification, as shown in Fig. 6 and Table 2. The SP-MFR-BiLSTM model has the advantage of increasing the exploitation process that selects the unique features and increases efficiency. The KNN model is sensitive to outliers that improve the performance, Random Forest (RF) has an overfitting problem and Support Vector Machine (SVM) model has imbalance data problem. The LSTM model has vanishing gradient problem and SP-MRF model increases the efficiency of classification. The SP-MRF-BiLSTM model has 99.97 % accuracy, 99.52 % sensitivity, and LSTM has 98.7 % accuracy and 97.3 % accuracy.

The SP-MFR-BiLSTM is compared with existing methods in PVC classification, as given in Table 3. The SP-MFR-BiLSTM model has higher efficiency than existing methods in PVC classification due to its efficiency in spiral search. The KNN deep metric [14] model has a second higher performance due to CNN based feature extraction. The OTSU-Gamma [12] and Hybrid feature extraction model [11] has considerable performance in PVC classification. The existing methods [11, 12, 14] have lower sensitivity and sensitivity is an important measure in the medical system. The SP-MRF-BiLSTM model selects unique features to improve the efficiency and sensitivity of the model due to the spiral search process. The spiral search method can distinguish more similar features spiral search that helps to select unique features in the model. The SP-MFR-BiLSTM model has 99.97 % accuracy, and 99.52 % sensitivity, and the KNN-deep metric [14] has 99.59 % accuracy and 96.7 % sensitivity in the model.

6. Conclusion

The existing methods in PVC classification have the limitations of lower sensitivity due to the presence of more similar features. This research proposes the SP-MRF-BiLSTM model to increase the exploitation in the search process and improve performance. The SP-MRF-BiLSTM model is evaluated using the MIT-BIH dataset and compared with existing models. The spiral search technique can distinguish features related to the classes and select unique features for classification. The selected features were applied to the BiLSTM model to increase the classification performance. The existing KNN model is sensitive to an outlier in the data and the SVM model has imbalance data problem. Existing WOA and GO methods provide more priority to local features involved in local optima trap. The SP-MFR-BiLSTM model has 99.97 % accuracy, 99.52 % sensitivity, and KNN-deep metric has 99.59 % accuracy and 96.7 % sensitivity in the model. The future work of this model involves in applying the batch normalization based CNN model to improve classification performance.

Conflicts of Interest

The authors declare no conflict of interest.

Symbols	Description
$a_{i,j}$	corresponding activation
b	logarithmic spiral shape constant
b_0, b_c, b_f	Bias
c_{t-1}	LSTM unit last state
$\widetilde{c_t}$	candidate memory cell
c_t	cell value memory
D	Distance
f	non-linear function
f_t	forget gate
$\overleftarrow{h}$	backward layers
$\vec{h}$	Hidden unit function
h_{t-1}	cell output of previous step
h_t	cell output
i, j	Neuron
i_t	input gate
l	random number
o_t	output gate
$w_{m,n}$	convolution weight matrix
W_0, W_c, W_f, W_i	weight matrix
$X_{i,j}$	Manta Ray positions
$x_{i+m,j+n}$	upper neurons
X_{best}	best location
x_t	input data at time t

Author Contributions

Author 1: Data collection, concept, analysis, methodology, writing—original draft preparation, software, and writing—review, and editing. Author 2: The supervision, review, investigation. Author 3: Supervision, validation, review, investigation, and writing—review and editing

References

[1] M. R. A. Mahfuz, M. A. Moni, P. Lio, S. M. S. Islam, S. Berkovsky, M. Khushi, and J. M. Quinn, "Deep convolutional neural networks based ECG beats classification to diagnose cardiovascular conditions", *Biomedical Engineering Letters*, Vol. 11, No. 2, pp. 147-162, 2021.

[2] W. Ullah, I. Siddique, R. M. Zulqarnain, M. M. Alam, I. Ahmad, and U. A. Raza, "Classification of Arrhythmia in Heartbeat Detection Using Deep Learning", *Computational Intelligence and Neuroscience*, Vol. 2021, pp. 1-13, 2021.

[3] B. M. Mathunjwa, Y. T. Lin, C. H. Lin, M. F. Abbod, M. Sadrawi, and J. S. Shieh, "ECG Recurrence Plot-Based Arrhythmia Classification Using Two-Dimensional Deep Residual CNN Features", *Sensors*, Vol. 22, No. 4, p. 1660, 2022.

[4] Y. Lu, M. Jiang, L. Wei, J. Zhang, Z. Wang, B. Wei, and L. Xia, "Automated arrhythmia classification using depthwise separable convolutional neural network with focal loss", *Biomedical Signal Processing and Control*, Vol. 69, p. 102843, 2021.

[5] F. Akdeniz, İ. Kayikcioglu, and T. Kayikcioglu, "Classification of cardiac arrhythmias using Zhao-Atlas-Marks time-frequency distribution", *Multimedia Tools and Applications*, Vol. 80, No. 20, pp. 30523-30537, 2021.

[6] W. Zeng and C. Yuan, "ECG arrhythmia classification based on variational mode decomposition, Shannon energy envelope and deterministic learning", *International Journal of Machine Learning and Cybernetics*, Vol. 12, No. 10, pp. 2963-2988, 2021.

[7] A. Y. Tan, K. Elharrif, R. C. Guarache, P. Mankad, O. Ayers, M. Joslyn, A. Das, K. Kaszala, S. F. Lin, K. A. Ellenbogen, and A. J. Minisi, "Persistent Proarrhythmic Neural Remodeling Despite Recovery From Premature Ventricular Contraction-Induced Cardiomyopathy", *Journal of the American College of Cardiology*, Vol. 75, No. 1, pp. 1-13, 2020.

[8] T. Yamada, "Twelve-lead electrocardiographic localization of idiopathic premature ventricular contraction origins", *Journal of Cardiovascular Electrophysiology*, Vol. 30, No. 11, pp. 2603-2617, 2019.

[9] J. F. Huizar, A. Y. Tan, K. Kaszala, and K. A. Ellenbogen, "Clinical and translational insights on premature ventricular contractions and PVC-induced cardiomyopathy", *Progress in Cardiovascular Diseases*, Vol. 66, pp. 17-27, 2021.

[10] B. R. D. Oliveira, C. C. E. D. Abreu, M. A. Q. Duarte, and J. V. Filho, "Geometrical features for premature ventricular contraction recognition with analytic hierarchy process based machine learning algorithms selection", *Computer Methods and Programs in Biomedicine*, Vol. 169, pp. 59-69, 2019.

[11] M. S. Memon, A. Lakhan, M. A. Mohammed, M. Qabulio, F. A. Turjman, and K. H. Abdulkareem, "Machine learning-data mining integrated approach for premature ventricular contraction prediction", *Neural Computing and Applications*, Vol. 33, No. 18, pp. 11703-11719, 2021.

[12] L. H. Wang, L. J. Ding, C. X. Xie, S. Y. Jiang, I. C. Kuo, X. K. Wang, J. Gao, P. C. Huang, P. A. and P. A. R. Abu, "Automated Classification Model With OTSU and CNN Method for Premature Ventricular Contraction Detection", *IEEE Access*, Vol. 9, pp. 156581-156591, 2021.

[13] N. T. Sarshar and M. Mirzaei, "Premature Ventricular Contraction Recognition Based on a Deep Learning Approach", *Journal of Healthcare Engineering*, Vol. 2022, pp. 1-7, 2022.

[14] J. Yu, X. Wang, X. Chen, and J. Guo, "Automatic Premature Ventricular Contraction Detection Using Deep Metric Learning and KNN", *Biosensors*, Vol. 11, No. 3, p. 69, 2021.

[15] H. Yang and Z. Wei, "A Novel Approach for Heart Ventricular and Atrial Abnormalities Detection via an Ensemble Classification Algorithm Based on ECG Morphological Features", *IEEE Access*, Vol. 9, pp. 54757-54774, 2021.

[16] E. H. Houssein, I. E. Ibrahim, N. Neggaz, M. Hassaballah, and Y. M. Wazery, "An efficient ECG arrhythmia classification method based on Manta ray foraging optimization", *Expert Systems with Applications*, Vol. 181, p. 115131, 2021.

[17] W. Zhao, Z. Zhang, and L. Wang, "Manta ray foraging optimization: An effective bio-inspired optimizer for engineering applications",

Engineering Applications of Artificial Intelligence, Vol. 87, p. 103300, 2020.

[18] J. Feng, X. Luo, M. Gao, A. Abbas, Y. P. Xu, and S. Pouramini, "Minimization of energy consumption by building shape optimization using an improved Manta-Ray Foraging Optimization algorithm", *Energy Reports*, Vol. 7, pp. 1068-1078, 2021.

[19] T. Chen, R. Xu, Y. He, and X. Wang, "Improving sentiment analysis via sentence type classification using BiLSTM-CRF and CNN", *Expert Systems with Applications*, Vol. 72, pp. 221-230, 2017.

[20] G. Xu, Y. Meng, X. Qiu, Z. Yu, and X. Wu, "Sentiment Analysis of Comment Texts Based on BiLSTM", *IEEE Access*, Vol. 7, pp. 51522-51532, 2019.

[21] R. Mark and G. Moody, "MIT-BIH arrhythmia database directory", *Cambridge: Massachusetts Institute of Technology*, 1988.